Angular Distribution of Charge Exchange and Inelastic Neutrons in π^--p Interactions at 313 and 371 MeV*

DON L. LIND,† BARRY C. BARISH,‡ RICHARD J. KURZ,§
PHILIP M. OGDEN,‖ AND VICTOR PEREZ-MENDEZ
Lawrence Radiation Laboratory, University of California, Berkeley, California

(Received 11 February 1965)

Neutron angular distributions from the charge-exchange ($\pi^0 n$) and inelastic modes ($\pi^0\pi^0 n$, $\pi^+\pi^- n$) of the π^--p interaction have been investigated at 313 and 371 MeV incident-pion kinetic energy. The data were obtained with an electronic counter system. Elastic and inelastic neutrons were separated in the all-neutral final states by time of flight. At both energies the charge-exchange differential cross section at the forward neutron angles differs from that determined by Caris *et al.* from measurements of the π^0-decay gamma distributions, but generally agrees with the phase-shift-analysis calculations of Roper. The distribution of inelastic neutrons from both modes shows a strong preference for low center-of-mass neutron energies. The distribution of these neutrons does not correspond to that expected from the $I=0$, π-π interaction (ABC effect) suggested to account for the anomaly in p-d collisions observed by Abashian *et al.* Finally, all available charge-exchange differential-cross-section data from this and other experiments were combined by a least-squares fit to a Legendre expansion of the form

$$\frac{d\sigma}{d\Omega^*}(\cos\theta_{\pi^0}^*)=\sum_{l=0}^{N} a_l P_l(\cos\theta_{\pi^0}^*)$$

with the following results (in mb/sr):

T_{π^-}	a_0	a_1	a_2	a_3
313	1.21±0.03	1.88±0.06	1.61±0.06	0.45±0.06
371	0.89±0.02	1.57±0.04	1.13±0.04	0.38±0.03.

I. INTRODUCTION

THE angular distribution of final-state neutrons occurring in π^--p collisions in the 300–400-MeV energy range provides insight into two different aspects of the pion-nucleon interaction. First, the distribution of elastic neutrons (from the reaction $\pi^- p \rightarrow \pi^0 n$) measures directly the differential cross section for this charge-exchange reaction. Secondly, the angular distribution of the inelastic neutrons (from $\pi^- p \rightarrow \pi^0\pi^0 n$ and $\pi^- p \rightarrow \pi^-\pi^+ n$) provides information about the isotopic state $I=0$ of the two pions occurring in these inelastic reactions.

At 310 MeV considerable effort has been made to determine an unambiguous phase-shift solution for pion-nucleon scattering. Foote *et al.*,[1] and Rogers *et al.*[2] have made a very accurate determination of π^+-p differential cross sections and recoil-proton polarization at this energy. Rugge and Vik[3] have provided similarly accurate cross-section and polarization data for $\pi^- p$ elastic scattering and have proposed various phase-shift solutions which fit all these data.[4]

The inclusion of corresponding data in this phase-shift analysis from the charge-exchange reaction has proven difficult. The only available charge-exchange differential-cross-section data were those measured by Caris *et al.*[5] at 317 MeV. However, when the Caris data were compared with charge-exchange distributions predicted by phase-shift solutions determined with the elastic-scattering differential-cross-section and polarization data,[4] it was apparent that there was considerable deviation at the backward pion angles.

The charge-exchange distribution had not been measured directly. Because of the extremely short lifetime of the π^0 meson (2.2×10^{-16} sec), only the gamma rays into which it decays could be detected. From this observed gamma-ray spectrum, the π^0 angular distribution had to be deduced. When the original data analysis was made, the total cross sections for the other final states that contribute to the observed γ rays ($\pi^0\pi^0 n$ and $\pi^-\pi^0 p$) were insufficiently known to provide an accurate correction factor at backward pion angles. It was at these same backward angles that the phase-shift predictions of Vik and Rugge departed most from the charge-exchange data of Caris. In addition, charge-exchange data taken by Kurz[6] at 374 MeV appeared to differ sufficiently from corresponding observations made by Caris to be in significant disagreement. Therefore it was decided to conduct the present experiment to measure the charge-exchange

* Work done under the auspices of the U. S. Atomic Energy Commission.

† Present address: Goddard Space Flight Center, Greenbelt, Maryland.

‡ Present address: Synchrotron Laboratory, California Institute of Technology, Pasadena, California.

§ Present address: École Polytechnique, Paris, France.

‖ Present address: Seattle Pacific College, Seattle, Washington.

[1] J. Foote, O. Chamberlain, E. Rogers, H. Steiner, C. Wiegand, and T. Ypsilantis, Phys. Rev. **122**, 948 (1961).

[2] E. H. Rogers, O. Chamberlain, J. Foote, H. Steiner, C. Wiegand, and T. Ypsilantis, Rev. Mod. Phys. **33**, 356 (1961).

[3] Hugo R. Rugge and Olav T. Vik, Phys. Rev. **129**, 2300 (1963).

[4] Olav T. Vik, and Hugo R. Rugge, Phys. Rev. **129**, 2311 (1963).

[5] J. C. Caris, R. W. Kenney, V. Perez-Mendez, and W. A. Perkins, Phys. Rev. **121**, 893 (1961).

[6] Richard J. Kurz, Ph.D. thesis, University of California Radiation Laboratory Report UCRL-10564, 1962 (unpublished).

TABLE I. Summary of π^- beam characteristics.

Energy (MeV)	ΔT (MeV)	Intensity (π/min)	Muon contamination (%)	Electron contamination (%)
313	14	25×10^6	5.8	0.3
371	13	12×10^6	4.0	0.3

differential cross section by observing the only directly accessible final-state particle—the neutron.

The inelastic neutrons, which we had to identify and separate from the elastic-neutron differential-cross-section data, occur in association with two-pion final states which contain the isotopic eigenstate $I=0$. An enhancement of two-pion production in this $I=0$ state has been proposed as an explanation for the anomalous bump in the He^3 momentum spectrum arising from high-energy proton-deuterium collisions as observed by Abashian *et al.*[7,8] (the so-called ABC effect).

If such an enhancement occurs it would alter the distribution of inelastic neutrons. However, two groups at Berkeley[6,9] have looked at two-pion final states ($\pi^-\pi^+n$ and $\pi^0\pi^0n$) in pion-nucleon collisions and have not observed any clear evidence for such a two-pion interaction. Therefore in the present experiment an analysis of the inelastic neutron distribution was included to provide further information on this question.

Sections II and III discuss briefly the experimental method and data analysis involved in this experiment. This is discussed more completely in Ref. 10. Section IV presents the results of both the elastic- and inelastic-neutron measurements. In this last section we also discuss the angular distribution which we derive for the charge-exchange reaction by combining the elastic-neutron data from this experiment with the other available data for this reaction.

II. EXPERIMENTAL METHOD

The collision of a negative pion at 313- or 371-MeV laboratory kinetic energy and a proton at rest provides sufficient energy to open some of the inelastic channels of the πN system with the production of an additional final-state pion. Although the higher of these energies is above the threshold for the production of two pions, these contributions are assumed to be negligibly small. Thus we must detect and separate the products of the following reactions:

$$\pi^-+p\rightarrow\pi^-+p \quad \text{elastic scattering,} \quad (1)$$

$$\pi^-+p\rightarrow\pi^0+n \quad \text{charge exchange,} \quad (2)$$

$$\pi^-+p\rightarrow\gamma+n \quad \text{radiative absorption,} \quad (3)$$

$$\left.\begin{aligned}&\pi^-+p\rightarrow\pi^0+\pi^0+n \quad (4)\\ &\pi^-+p\rightarrow\pi^-+\pi^++n \quad (5)\\ &\pi^-+p\rightarrow\pi^-+\pi^0+p \quad (6)\end{aligned}\right\}\ \text{pion production,}$$

$$\pi^-+p\rightarrow\pi^-+\gamma+p \quad \text{nuclear bremsstrahlung.} \quad (7)$$

A detector accepting only neutral particles will signal the presence of a neutron (since gamma rays can be distinguished from neutrons, as we show) and will eliminate reactions (1), (6), and (7). The cross section for radiative absorption (3) is small compared to other neutron sources, so these neutrons can be treated as a mathematical correction to the data. By detecting any charged pions in coincidence with a neutron, reaction (5) can be identified and counted separately. The inelastic neutrons of reaction (4) emerge from the target with a spectrum of energies. At a fixed lab-system angle, the highest of these energies is less than the unique energy of the elastically scattered charge-exchange neutrons (2). This gives a separation between their velocities. Thus, the neutrons from reactions (2) and (4) can be separated by their time-of-flight over a measured path length.

The negative pion beam was produced when the internal 732-MeV proton beam of the Berkeley 184-in. synchrocyclotron struck an internal beryllium target 2 in. thick in the beam direction. The pions were deflected outwardly by the magnetic field of the cyclotron. Their trajectory was calculated by the computer program CYCLOTRON ORBITS,[11] which uses measured values of the cyclotron magnetic field to integrate the equations of motion of the particle. A beam transport system consisting of two doublet quadrupole magnets and a momentum-analyzing bending magnet focused the pion beam on the liquid-hydrogen target. The current settings of these magnets were determined by the beam-optics computer program, OPTIK[12] and by suspended-wire measurements. The angle of deflection in the bending magnet was chosen to produce a recombination at the final image of the momentum dispersion introduced by the cyclotron field. The average energy and energy spread of the beam were experimentally checked by integral range measurements in Cu. The μ^- contamination of the beam due to π^- decays before the bending magnet was determined from these range curves. μ^- production beyond this magnet was calculated and combined with the range-curve information

[7] Alexander Abashian, Norman E. Booth, and Kenneth M. Crowe, Phys. Rev. Letters **5**, 258 (1960); Norman E. Booth, Alexander Abashian, and Kenneth M. Crowe, *ibid.* **7**, 35 (1961).

[8] Alexander Abashian, Norman E. Booth, Kenneth M. Crowe, Roger E. Hill, and Ernest H. Rogers, Phys. Rev. **132**, 2296, 2305; 2309; 2314 (1963).

[9] Janos Kirz, Joseph Schwartz, and Robert D. Tripp, Phys. Rev. **130**, 2481 (1963).

[10] Don L. Lind, Ph.D. thesis, University of California Radiation Laboratory Report UCRL-11435 1964 (unpublished).

[11] Joe Good, Morris Pripstein, and Howard S. Goldberg, University of California Radiation Laboratory Report UCRL-11044 1963 (unpublished).

[12] Thomas J. Devlin, University of California Radiation Laboratory Report UCRL-9727, 1961 (unpublished).

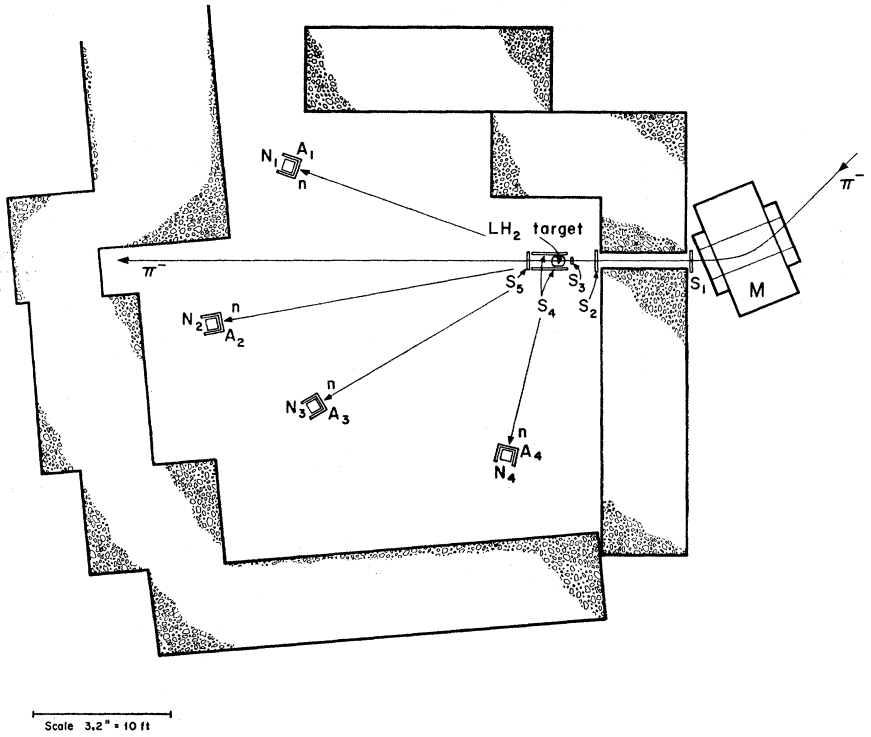

FIG. 1. Plan view of the experimental area showing target and counter arrangement.

to give the total μ^- contamination. The electron contamination was estimated from gas Čerenkov-counter measurements on similar beams. The properties of the pion beam are listed in Table I.

Figure 1 shows the arrangement of the experimental area beyond the bending magnet M. Located along the pion beam are four scintillation counters (S_1, S_2, S_3, and S_5), which form the beam-monitoring system. Surrounding the hydrogen target is a cylindrical counter (S_4) used to detect charged pions. The four neutron counters (N_{1-4} surrounded by anticoincidence counters A_{1-4}) are located at representative positions for detecting neutral particles originating in the target.

Counters S_1, S_2, and S_3 were located in the beam to monitor the incident-pion flux arriving at the target position. The smallest counter S_3 defined the area of the beam accepted by the monitor system. S_2 served as the source of the zero-time signal for the time-of-flight analysis. Counter S_5, located beyond the hydrogen target and used in anticoincidence, rejected incident pions that were not scattered by an angle greater than 10 deg in the hydrogen. Counter S_4 detected the presence of one or both of the charged pions in coincidence with a neutron from reaction (5). Thus these "charged mode" neutron events could be recorded separately from the "neutral mode" events [reactions (2) or (4)].

Neutrons were detected in a block of plastic scintillator by observing the light produced by recoiling charged products arising in interactions between the incident neutrons and the hydrogen and carbon nuclei of the scintillator. Gamma rays were similarly registered by the counter, but these could be clearly distinguished by their earlier arrival time. The scintillator block was 4 in. thick in the direction of neutron penetration, and had an octagonal frontal area formed by removing the corners of a 4×10-in. rectangle. An Amperex 58 AVP phototube with a photocathode $5\frac{1}{4}$ in. in diameter was used in order to obtain efficient light collection from the large block of scintillator.

Each detector was surrounded by an anticoincidence counter which was shaped as an octagonal box completely surrounding the scintillator block and extending back an additional 4 in. beyond the sensitive area. The front face and sides of this counter were formed of $\frac{1}{4}$-in. plastic scintillator, and were viewed by two RCA 6810A phototubes whose signals were added. The efficiency of the counter to reject charged particles was estimated as >99.5%. The four neutron detectors recorded data simultaneously, from positions on both sides of the π^- beam, and at laboratory angles from 10 to 60 deg. The neutron flight path was set at 3, 4, or 5 m, depending on the angle.

For the time-of-flight analysis the signal from scintillator S_2 was used as the "start" signal for a time-to-height converter. The "stop" signal was generated when a neutral particle registered in one of the neutron detectors. This neutron-timing information was obtained from the phototube signal by pulse differentiation with an overdamped LC-tuned circuit to produce a zero-crossing signal whose zero-crossing point was detected by a tunnel-diode discriminator. This tech-

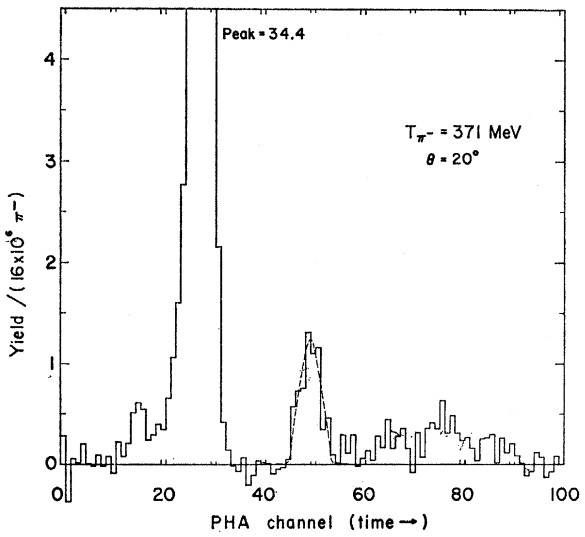

FIG. 2. Neutral-mode time-of-flight spectra. The solid-line histogram is the neutral-particle yield. The dashed line is a Gaussian curve fitted to the elastic-neutron peak. (The detailed structure of the spectra is discussed in the text.)

nique was used because the time shift of the output pulse is very small over a large dynamic range of photomultiplier-input light levels.[13] Events were routed according to whether they were "neutral" or "charged" mode and counted in a pulse-height analyzer (PHA).

Figure 2 shows a PHA record, after all runs for a particular experimental condition had been combined. The yield is shown as a function of PHA channel number which is proportional to the time of flight from the target to the detector. The first particles to arrive are the γ rays, which form the large peak centered at channel 27. These are clearly distinguishable from the elastic neutrons that arrived next and formed the peak at channel 50. Finally the slower inelastic neutrons are distributed over the next 30 or so channels. Figure 2 was chosen to illustrate the worst situation we encountered in separating the elastic from the inelastic neutrons. At this particular laboratory angle, pion energy, and flight-path distance, the statistical fluctuations due to the low yield leave the least distinguishable "valley" between the two types of neutrons. Still, at this most adverse condition, we were able to unambiguously fit the elastic-neutron peak with a Gaussian curve whose area represents the total-elastic-neutron yield at this angle. Analysis of the gamma peak showed the timing resolution of the entire system to be about 1.5 nsec.

III. DATA ANALYSIS

Before the differential cross sections could be calculated from the neutron yields it was necessary to normalize these yields by the following corrections.

[13] Arthur E. Bjerke, Quentin A. Kerns, and Thomas A. Nunamaker, University of California Radiation Laboratory Report UCRL-9838, 1961 (unpublished).

1. Neutron-Detection Efficiency

The neutron-detection efficiency of plastic scintillator is a function of neutron energy, the threshold for the detection of scintillation light, and the detector geometry. A computer program called TOTEFF[14] was used to compute the neutron-detection efficiency as a function of neutron energy for each of the two detection thresholds at which data were taken.

The efficiency varies between 0.07 and 0.17 with an uncertainty of $\pm 10\%$. This is regarded as an upper limit and it determines the over-all uncertainty of the data. The efficiency values obtained from this program are compatible with corresponding measurements made by Wiegand *et al.*[15]

2. Gamma Conversion

Neutral pion mesons occur as final-state particles in both reactions (2) and (4). If the γ rays into which these mesons decay produce e^+, e^- pairs in the target walls, or if the neutral pion decays in the $\pi^0 \rightarrow \gamma e^- e^+$ mode, and one of the charged particles passes through scintillation counter S_5, the event would be lost. This turns out to be a negligible effect. However, if one of the charged particles is detected by S_4, the accompanying neutron would be misconstrued as having arisen from reaction (5). The probability of such a gamma conversion and its subsequent detection was calculated as a function of the laboratory angle of the associated neutron.[10] "Neutral" mode data were increased and "charged" mode data were decreased by this correction.

3. Neutron Rescattering and Absorption

After the initial-scattering process in which they are produced, the neutrons can interact with nuclei in the material immediately surrounding the target. This can be either by elastic rescattering, in which case no neutrons would be lost, but the differential distribution of the neutrons might be altered; or the neutrons could interact inelastically with the target nuclei and be absorbed, decreasing the apparent flux at the neutron detectors. The qualitative behavior of rescattering is to shift the elastic-neutron distribution toward the smaller angles where the cross section is lowest. However, even the most adverse assumptions indicated that such a shift would be less than the uncertainty of the neutron-detection-efficiency calculation. In absorption reactions such as $C^{12}(n,\alpha)Be^9$ and $Al^{27}(n,p)Mg^{27}$, no neutrons exist in the final state. A calculation was made of the decrease in the neutron flux due to these inelastic processes.[10] This attenuation varies as a function of neutron laboratory angle due to the changes in neutron energy, as well as the varying amount of material

[14] Richard J. Kurz, University of California Radiation Laboratory Report UCRL-11339, 1964 (unpublished).

[15] Clyde E. Wiegand, Tom Elioff, William B. Johnson, Leonard B. Auerbach, Joseph Lach, and Thomas Ypsilantis, University of California Radiation Laboratory Report UCRL-9986, 1961 (unpublished).

TABLE II. $\pi^- p \rightarrow \pi^0 n$ angular distribution data for various values (in MeV) of T_{π^-} [(a), (b), (c), and (d) refer to the designations in Sec. IV of the text].

(a)		(b)		(c)		(d)	
$\cos\theta_n^*$	$d\sigma/d\Omega^*$ (mb/sr)	$\cos\theta_n^*$	$d\sigma/d\Omega^*$ (mb/sr)	$\cos\theta_\gamma^*$	$d\sigma^\gamma/d\Omega^*$ (mb/sr)	$\cos\theta_{\pi^0}^*$	$d\sigma/d\Omega^*$ (mb/sr)
313 MeV				317 MeV		315 MeV	
−0.536	1.77±0.20			1.000	2.80±0.20	1.000	4.30±0.57
−0.385	1.40±0.14			0.889	2.44±0.15		
−0.222	0.73±0.07			0.779	2.18±0.14		
−0.050	0.44±0.04			0.598	1.64±0.11		
0.125	0.27±0.03			0.225	0.80±0.06		
0.297	0.23±0.02			−0.199	0.29±0.05		
0.461	0.27±0.03			−0.589	0.21±0.04		
0.612	0.32±0.04			−0.869	0.39±0.04		
0.745	0.37±0.04			−0.952	0.31±0.05		
0.853	0.41±0.05						
0.933	0.46±0.10						
371 MeV		374 MeV		371 MeV		371 MeV	
		−0.678	1.69±0.17	1.000	2.59±0.17	1.000	3.65±0.65
−0.545	1.59±0.16	−0.545	1.31±0.13	0.970	2.25±0.15		
		−0.400	0.97±0.10	0.882	2.12±0.13		
−0.233	0.60±0.06	−0.233	0.62±0.06	0.766	1.84±0.11		
		−0.062	0.41±0.04	0.577	1.23±0.08		
0.113	0.22±0.02			0.194	0.60±0.05		
0.500	0.14±0.01			−0.230	0.23±0.04		
0.740	0.11±0.01			−0.610	0.14±0.05		
0.932	0.10±0.01			−0.877	0.05±0.05		
				−0.955	0.26±0.05		

encountered when the neutron leaves the target in various directions.

4. Radiative Absorption

Neutrons that originate in the radiative absorption reaction (3) cannot be resolved by time of flight, and must be subtracted from the events recorded in the neutral-mode data. This correction was obtained from a detailed-balance calculation involving the "complementary" reaction, pion photoproduction. The negative pion-photoproduction cross section was obtained from the negative-to-positive pion-photoproduction ratio from deuterium as measured by Neugebauer *et al.*[16] and the positive-pion-photoproduction cross sections of Walker *et al.*[17] and Tollestrup *et al.*[18]

IV. RESULTS

A. Elastic Neutrons

The charge-exchange differential cross sections were computed from the corrected elastic neutron yields and are shown in Fig. 3. For comparison with other work these results are plotted as a function of $\theta_{\pi^0}^*$=c.m. system pion angle=$180°-\theta_n^*$. (* denotes c.m. system variable.) These results are presented numerically in column (a) of Table II. This data covers the range $21 \leqslant \theta_n^* \leqslant 123$ deg. Also shown in Table II are three other classes of data which we have incorporated in an analysis of the angular distribution of reaction (2): column (b) neutron differential cross section at an

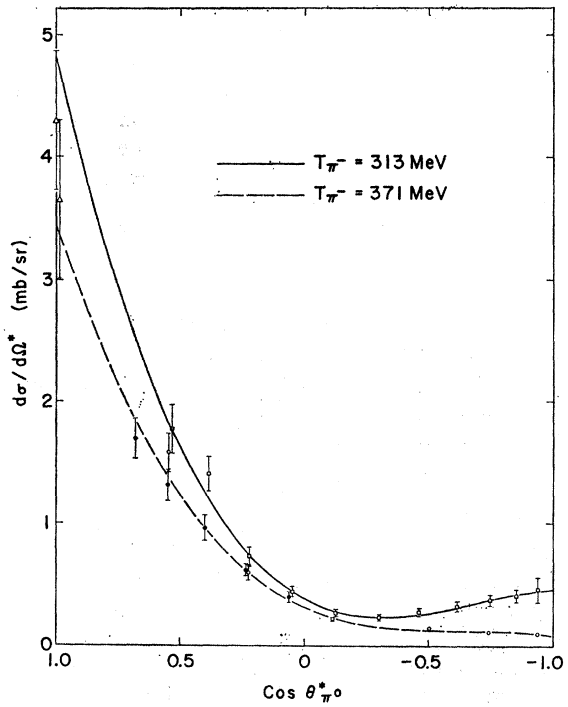

FIG. 3. Charge-exchange differential cross section at T_{π^-}=313 and 371 MeV. (□) Measured in this experiment (313 MeV); (○) measured in this experiment (371 MeV); (●) measured by Kurz (374 MeV); (△) forward-dispersion-relation calculation. Curves are least-squares fits to the data.

[16] Gerry Neugebauer, Walter Wales, and R. L. Walker, Phys. Rev. **119**, 1726 (1960).
[17] R. L. Walker, J. G. Teasdale, V. Z. Peterson, and J. A. Vette, Phys. Rev. **99**, 210 (1955).
[18] A. V. Tollestrup, J. Ç. Keck, and R. M. Worlock, Phys. Rev. **99**, 220 (1955).

TABLE III. Results of the least-squares fits of the differential cross section for $\pi^- p \to \pi^0 n$ to the form

$$\frac{d\sigma}{d\Omega^*}(\cos\theta_{\pi^0}^*) = \sum_{l=0}^{N} a_l P_l(\cos\theta_{\pi^0}^*).$$

T_{π^-} (MeV)		N	a_0	a_1	a_2 (mb/sr)	a_3	Probability of fit
315	a	2	1.31±0.04	1.86±0.08	1.57±0.11	···	0.57
	b	2	0.92±0.04	1.17±0.08	0.96±0.07	···	10^{-3}
		3	1.13±0.06	1.73±0.14	1.50±0.13	0.44±0.09	0.88
	c	2	1.16±0.03	1.62±0.05	1.31±0.05	···	$<10^{-4}$
		3	1.21±0.03	1.88±0.06	1.61±0.06	0.45±0.06	0.40
371	a	2	1.00±0.03	1.62±0.06	1.12±0.08	···	0.15
	b	2	0.60±0.02	0.89±0.05	0.44±0.03	···	$<10^{-4}$
		3	0.80±0.03	1.37±0.08	0.96±0.07	0.31±0.04	0.75
	c	2	0.77±0.02	1.26±0.03	0.67±0.02	···	$<10^{-4}$
		3	0.89±0.02	1.57±0.04	1.13±0.04	0.38±0.03	0.12

[a] γ data only.
[b] Neutron data and forward-direction dispersion-relation point.
[c] All data combined.

incident pion kinetic energy $T_{\pi^-}=374$ MeV in the range $84 \leqslant \theta_n^* \leqslant 133$ deg,[6] (c) previously published angular distributions at $T_{\pi^-}=317$ and 371 MeV;[5] and (d) the differential cross section at $\theta_{\pi^0}^*=0$ deg calculated from forward-direction, fixed-momentum-transfer dispersion relations for pion nucleon scattering.[19] A least-squares analysis was performed to fit these data to the c.m. system differential cross section in the form:

$$\frac{d\sigma}{d\Omega^*}(\cos\theta_{\pi^0}^*) = \sum_{l=0}^{N} a_l P_l(\cos\theta_{\pi^0}^*). \tag{8}$$

The γ data were incorporated into the least-squares analysis according to the procedure used by Caris *et al.*[5] If $d\sigma/d\Omega^*$ is represented as in Eq. (8), the expected experimental γ angular distribution in the c.m. system, taking into the account the γ detection efficiency of the experimental system, is given by

$$\frac{d\sigma^\gamma}{d\Omega^*}(\cos\theta_\gamma^*) = \sum_{l=0}^{N} a_l P_l(\cos\theta_\gamma^*) \int_{-1}^{1} \frac{dx\, P_l(x)\epsilon(k)}{(\gamma-\eta x)^2}, \tag{9}$$

where x is the cosine of the angle between the photon and the π^0 in the c.m. system, γ and η denote the motion of the π^0 rest system with respect to the c.m. system, and $\epsilon(k)$ is the γ-detector efficiency as a function of the photon lab-system energy, k, which in turn is a function of x and $\cos\theta_\gamma^*$.

The present analysis started with the uncorrected data of Caris *et al.* (see Table IV, Ref. 5). The correction of the observed distributions to take into account photons originating from the reactions $\pi^- p \to \pi^0\pi^0 n$ and $\pi^-\pi^0 p$ was reperformed. The availability of more precise information on these reactions made a more accurate estimation of the correction feasible.[20] For each reaction we assume that the π^0's had an invariant phase-space energy distribution and an isotropic angular distribution in the c.m. system. We calculated the corresponding lab-system distribution of photons in energy and angle, $d^2\sigma/dkd\Omega$, with a normalization determined by the total cross sections for the $\pi^0\pi^0 n$ and $\pi^-\pi^0 p$ reactions. To obtain the values of $d\sigma^\gamma/d\Omega^*$ used in this analysis, we subtracted the quantity

$$\frac{d\sigma^{\text{inel}}}{d\Omega}(\theta_\gamma) = \int dk \frac{d^2\sigma(k,\theta_\gamma)}{dkd\Omega}\epsilon(k) \tag{10}$$

from the uncorrected data points of Caris *et al.* We used their original values for the remaining corrections that they discuss. The values used in the least-squares analysis are given in Table II column (c).

The neutron data provided information on the portion of the angular distribution in which the uncertainties in the γ data are greatest. The relative magnitude of the calculated corrections to the γ-angular distribution is greater for $\theta_\gamma^* > 90$ deg. In addition, the statistical weight of the γ data is lowest in this region.

We performed the least-squares analysis with (a) the recorrected γ data alone, (b) the neutron data and the dispersion-relation points, and (c) all data simultaneously. The results are given in Table III. At $T_{\pi^-}=315$ (the average T_{π^-} for the various data) and 371 MeV the probability of fit was not significantly increased for $N>2$ for case (a) and for $N>3$ for cases (b) and (c). At $T_{\pi^-}=315$ MeV for case (c) the γ-data point at $\cos\theta_\gamma^* = -0.955$ was deleted since the inclusion of this point decreased the probability of fit to 0.001.

The differential cross section for $\pi^- p \to \pi^0 n$ at $T_{\pi^-}=315$ and 371 MeV as determined by the least-squares analysis of the recorrected γ data and by the analysis of the combined data are plotted in Fig. 4. The nonzero value of a_3 obtained in the combined data analysis is consistent with the requirement of at least D waves in other analyses of pion-nucleon interactions at $T_{\pi^\pm}=310$ MeV.[4] However, the behavior of the angular distribution in the region of $\theta_{\pi^0}^*=180$ deg is not

[19] David Cheng, Lawrence Radiation Laboratory, Berkeley, 1964 (private communication).
[20] Barry C. Barish, Richard J. Kurz, Victor Perez-Mendez, and Julius Solomon, Phys. Rev. **135**, B416 (1964).

consistent with any of the *SPD* solutions of Vik and Rugge. The same comment applies to the results of measurements of the neutron polarization in $\pi^- p \to \pi^0 n$ at $T_{\pi^-}=310$ MeV.[21] The differential cross section obtained here corresponds most closely to predictions obtained from *SPDF* solutions II and IV of Vik and Rugge.[22] We note that the *SPDF* solution II of Vik and Rugge is preferred by the recent theoretical analysis of pion-nucleon scattering of Donnachie *et al.*[23] The angular distribution at $T_{\pi^-}=315$ and 371 MeV presented here deviates from that determined from the γ data alone in a manner which is in agreement with the predictions of an energy-dependent phase-shift analysis of pion-nucleon scattering by Roper.[22,24] The predictions by Roper at $T_{\pi^-}=310$ and 370 MeV are also plotted in Fig. 4. He used the data of Caris *et al.* in his analysis as well as all other available data on pion-nucleon scattering (including the neutron polarization data referred to above). At both energies, $d\sigma/d\Omega^*$ for $\theta_{\pi^0}^*<90$ deg is lower than the predictions by Roper. At $\theta_{\pi^0}^*=180$ deg, isotopic spin considerations place a lower limit on $d\sigma/d\Omega$ for $\pi^- p \to \pi^0 n$ in terms of the differential cross sections for $\pi^\pm p \to \pi^\pm p$ at $\theta_\pi=180$ deg:

$$\frac{d\sigma^0}{d\Omega} \geqslant \tfrac{1}{2}\left[\left(\frac{d\sigma^+}{d\Omega}\right)^{1/2}-\left(\frac{d\sigma^-}{d\Omega}\right)^{1/2}\right]^2. \tag{11}$$

If we use the available data on elastic scattering,[2,3,25] this limit is 0.77 ± 0.20 mb/sr at $T_{\pi^-}=310$ MeV and 0.13 ± 0.06 mb/sr at $T_{\pi^-}=370$ MeV. The values corresponding to the $N=3$, combined data of Table III are 0.50 ± 0.11 mb/sr and 0.07 ± 0.07mb/sr, respectively. Thus the present charge-exchange angular distributions $\theta_{\pi^0}^*=180$ deg are barely compatible with this limit.

By integration of the $d\Omega^*$ curve over $\cos\theta_{\pi^0}^*$, a value for the total cross section σ_T for the reaction (2) was obtained. These results are presented in Table IV and are calculated from the "combined" data Table III with $N=3$.

TABLE IV. Total charge-exchange cross section.

T_{π^-} (MeV)	σ_T (mb)
313	15.1±0.4
371	11.1±0.2

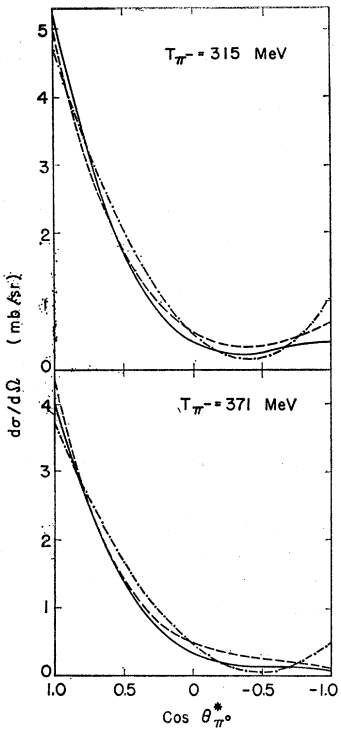

FIG. 4. Comparison of differential-cross-section data. (——) Combined neutron and gamma data; (—·—·) gamma data only; (– – –) differential cross section predicted by Roper phase-shift solutions.

B. Inelastic Neutrons

The inelastic-neutron distributions can be compared to phase-space distributions and distributions enhanced by an $I=0$ two-pion interaction, in either of two ways. The first is at a constant neutron angle. This would correspond to a vertical cut through the kinematically allowed inelastic area shown in Fig. 5. In effect, this is what is shown in the inelastic distribution in Fig. 2 except that the abscissa has been plotted as time-of-flight instead of neutron energy. The second possibility is at a constant neutron energy. This corresponds to a horizontal cut through the inelastic neutrons areas in Fig. 5. In this case an energy band can be selected sufficiently wide to avoid the statistical fluctuations seen in Fig. 2. In addition, since the neutron energy is constant, any inaccuracy in the neutron-detection efficiency is eliminated from the shape of the distribution. A calculation of the second type gives $d^2\sigma/dt\,d\Omega$ for constant T_N for both $\pi^+\pi^- n$ and $\pi^0\pi^0 n$ final states; this is presented numerically in Table V and graphically in Figs. 6 and 7. Also shown in the figures are the phase-space distribution and the distribution calculated by using an $I=0$ two-pion interaction enhancement factor with $a_0=2\mu^{-1}$ and $R=0$. This value of a_0 is the scattering length tentatively proposed by Abashian *et al.*[8] for the $I=0$ two-pion interaction, and $R=0$ is the radius of interaction. These curves are normalized to the integral of the distribution for $\pi^+\pi^- n$ over $\cos\theta$.

The distribution of inelastic neutrons from the $\pi^+\pi^- n$ final state departs noticeably from both the phase-space distribution and the ABC enhancement distribution.

[21] Roger E. Hill, Norman E. Booth, Robert J. Esterling, David L. Jenkins, Norman H. Lipman, Hugo R. Rugge, and Olav T. Vik, Bull. Am. Phys. Soc. **9**, 410 (1964).
[22] L. David Roper, Lawrence Radiation Laboratory, Livermore, 1964 (private communication).
[23] A. Donnachie, J. Hamilton, and A. T. Lea, Phys. Rev. **135**, B515 (1964).
[24] L. David Roper, Phys. Rev. Letters **12**, 340 (1964).
[25] Philip M. Ogden, Donald E. Hagge, Jerome A. Helland, Marcel Banner, Jean Francois Detoeuf, and Jacques Teiger, Phys. Rev. **137**, B1115 (1965).

TABLE V. Inelastic-neutron $d^2\sigma/dT\,d\Omega$ distribution at constant neutron energy.

T_{π^-} (MeV)	Cosθ_n	$d^2\sigma/dTd\Omega(\pi^+\pi^-n)$ (μb/MeV-sr)	$d^2\sigma/dTd\Omega(\pi^0\pi^0n)$ (μb/MeV-sr)
313	0.985	57.3±16.8	
	0.966		10.9±16.5
	0.959	33.5± 6.2	
	0.940		12.7±13.9
	0.906	16.0± 8.8	8.3±14.0
	0.866	11.7± 2.7	7.9± 3.9
	0.819	7.1± 2.7	3.6± 4.0
	0.766	6.7± 2.6	5.9± 4.3
371	0.985	60.1±11.0	18.7±10.7
	0.940	36.4± 5.5	20.0± 7.0
	0.866	15.2± 3.9	8.9± 4.4
	0.766	6.0± 2.8	0.4± 4.2

We observe that there is a strong peaking at low c.m. energy for the neutron. This same effect was observed by Kirz *et al.*,[9] Barish *et al.*,[20] and Blokhintseva *et al.*[26] These low-neutron energies correspond to a dipion effective mass in the range (near $m_{\pi\pi}=400$ MeV) where several authors report $I=0$ two-pion resonances.[27–29]

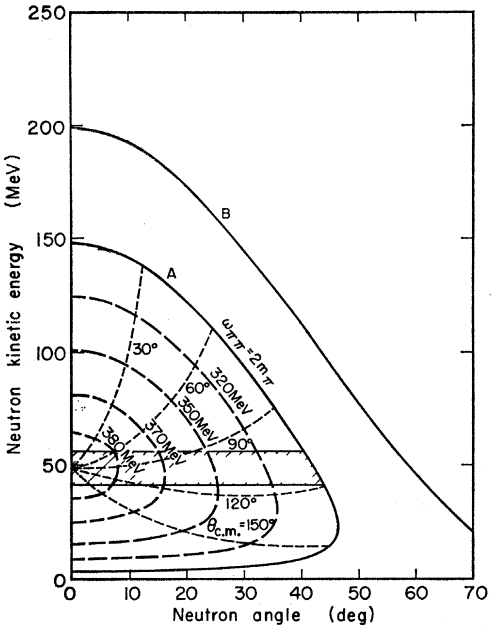

FIG. 5. Laboratory-system neutron kinematics for the processes $\pi^-p\to\pi\pi n$ (region inside curve A) and $\pi^-p\to\pi^0n$ (curve B) at 313 MeV. Curves at 371 MeV are similar. Shaded area is energy band used in inelastic-neutron analysis.

[26] T. D. Blokhintseva, V. G. Grebinnik, V. A. Zhukov, G. Libman, L. L. Nemenov, G. I. Selivanov, and Y. Jung-Fang, Zh. Eksperim. i Teor. Fiz. 44, 116 (1963) [English transl.: Soviet Phys.—JETP 17, 80 (1963)].

[27] N. P. Samios, A. H. Backman, R. M. Lea, T. E. Kalogeropoulos, and W. D. Shepard, Phys. Rev. Letters 9, 139 (1962).

[28] R. Del Fabbra, M. DePretis, R. Jones, G. Marini, A. Odian, G. Stoppini, and L. Tau, Phys. Rev. Letters 12, 674 (1964).

[29] C. Richardson, R. Kraemer, M. Meer, N. Nussbaum, A. Pevsner, R. Strand, T. Toohig and M. Block, in *Proceedings of the International Conference on High-Energy Nuclear Physics, Geneva, 1962*, edited by I. Prentki (CERN, Scientific Information Service, Geneva, Switzerland, 1962), p. 96.

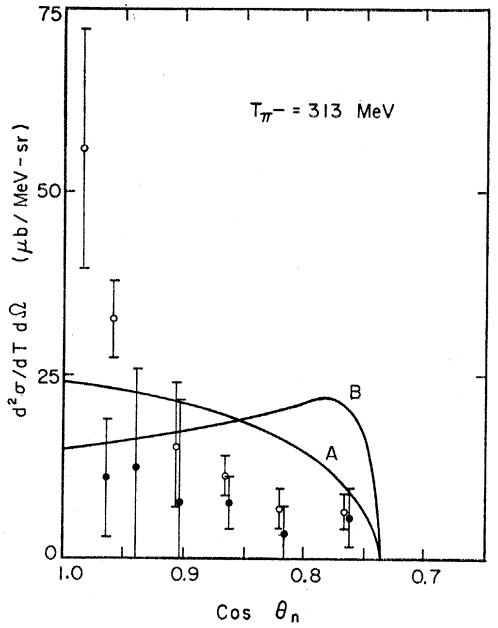

FIG. 6. Inelastic-neutron differential distribution for $T_{\pi^-}=313$ MeV (neutron energy interval from 42 to 57 MeV). (○) $d^2\sigma/dtd\Omega$ for $\pi^+\pi^-n$; (●) $d^2\sigma/dtd\Omega$ for $\pi^0\pi^0n$; (A) phase-space distribution; (B) distribution for $I=0$ two-pion interaction with $a_0=2\mu^{-1}$ and $R=0$.

This low-energy peaking seems to be present at $T_{\pi^-}=371$ MeV in the $\pi^0\pi^0n$ distribution, which is in agreement with Barish *et al.* but is not clearly evident at 313 MeV. However, at this energy the large statis-

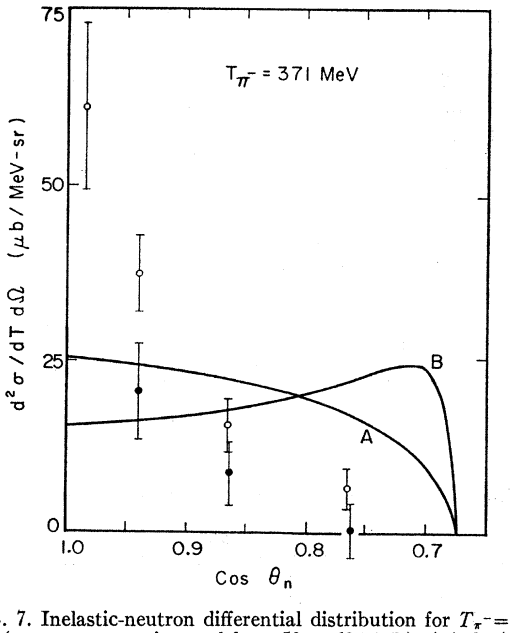

FIG. 7. Inelastic-neutron differential distribution for $T_{\pi^-}=371$ MeV (neutron energy interval from 50 to 69 MeV). (○) $d^2\sigma/dtd\Omega$ for $\pi^+\pi^-n$; (●) $d^2\sigma/dtd\Omega$ for $\pi^0\pi^0n$; (A) phase-space distribution; (B) distribution for $I=0$ two-pion interaction with $a_0=2\mu^{-1}$ and $R=0$.

tical errors of the data do not justify any firm conclusions.

The enhancement of the distribution from an $I=0$ two-pion interaction, which has been proposed to explain the anomaly observed by Abashian *et al.*[8] is not observed. However, the domination of the distribution by a strong enhancement at the opposite end of the neutron c.m. energy range may mask this effect. Finally we note that an explanation has been proposed by Anisovich and Dakhno for both of these enhancements in terms of a singularity in the scattering amplitude.[30]

[30] V. V. Anisovich and L. G. Dakhno, Phys. Letters **10**, 221 (1964).

ACKNOWLEDGMENTS

We would like to acknowledge the help, support, and encouragement received from Professor Burton J. Moyer thoughout the course of this experiment. We are indebted to Dr. Julius Solomon for his assistance in the beam-optics calculations and to Dr. L. David Roper for his helpful discussions and cooperation in transmitting the results of his phase-shift analysis. We are grateful to Dr. T. D. Spearman for pointing out the limit on charge-exchange differential cross sections at 180 deg. Finally we would like to thank James T. Vale and the members of the cyclotron crew for their help and cooperation during this experiment.

PHYSICAL REVIEW VOLUME 138, NUMBER 6B 21 JUNE 1965

Parametric Expression for p-p Off-Energy-Shell Matrix Elements and p-p Bremsstrahlung*

M. I. SOBEL†
Northeastern University, Boston, Massachusetts
(Received 3 February 1965)

An equation is derived which expresses the off-energy-shell matrix elements of the p-p interaction in a form analogous to the phase-shift expansion for elastic scattering. "Quasiphase parameters" which play the role of phase shifts in this expression are calculated from phenomenological potentials. p-p bremsstrahlung, with gamma rays observed perpendicular to the scattering plane of the incident proton, is discussed as a process which may permit experimental study of these parameters.

I. INTRODUCTION

In recent years a number of phenomenological potentials[1–4] have been proposed to represent the proton-proton interaction at energies up to 300 MeV. However, since these potentials were all fitted to elastic-scattering data,[5] only the on-energy-shell matrix elements of the interaction are directly determined. A complete understanding of the p-p interaction requires knowledge of the off-energy-shell elements as well. Recently proton-proton bremsstrahlung, at energies less than 300 MeV, was considered as an inelastic process which can be interpreted simply in terms of off-energy-shell elements.[6,7] The cross sections for this process, calculated using different phenomenological potentials, were found to differ by more than a factor of 2.

Since that time experimental effort at a number of laboratories has gone into the problem of nucleon-nucleon bremsstrahlung, and in two cases[8,9] preliminary results are available. It is therefore of interest to consider in a general way how the analysis of such experiments might proceed.

In Sec. II it is shown that the off-energy-shell matrix elements can be put in a form closely analogous to that for on-energy-shell elements. They have the same dependence on scattering angle, and involve energy-dependent quantities similar to phase shifts. These "quasiphase parameters" are then calculated for a number of phenomenological potentials. In Sec. III we discuss a particular choice of kinematics for p-p bremsstrahlung which is particularly useful for a detailed analysis of the matrix elements. For this process one can define not only a cross section, but also symmetry measurements for polarized incident beams. In Sec. IV some calculated values of these cross sections and polarizations are presented. Unfortunately, for the case considered, the polarizations turn out to be too small to be useful.

* Partially supported by grants from the National Science Foundation and the Army Research Office (Durham).
† Present address: Brooklyn College, Brooklyn, New York.
[1] K. A. Brueckner, J. A. Gammel, and R. M. Thaler, Phys. Rev. **109**, 1023 (1958).
[2] T. Hamada and I. D. Johnston, Nucl. Phys. **31**, 382 (1962).
[3] R. A. Bryan, Nuovo Cimento **16**, 895 (1960).
[4] K. E. Lassila, M. H. Hull, Jr., H. M. Ruppel, F. A. MacDonald, and G. Breit, Phys. Rev. **126**, 881 (1962).
[5] Michael J. Moravcsik, *The Two-Nucleon Interaction* (Clarendon Press, Oxford, England, 1963).
[6] M. I. Sobel and A. H. Cromer, Phys. Rev. **132**, 2698 (1963), hereafter referred to as SC.
[7] M. I. Sobel, Ph.D. thesis, Harvard University, 1964 (unpublished).
[8] B. Gottschalk (private communication).
[9] E. M. Thorndike, Kenneth W. Rothe, and Peter F. M. Koehler (private communication).